Malignant melanoma complicated with cataract and secondary glaucoma: A case report

YU WANG[1], QINQIN SUN[1], ZHIJIAN LI[1], FEI LENG[2], XUELIAN HAN[1], QIQI SU[1] and SHENG SU[1]

[1]Eye Hospital, The First Affiliated Hospital, Harbin Medical University, Harbin, Heilongjiang 150001, P.R. China;
[2]Department of Ophthalmology, Beijing Children's Hospital Affiliated with Capital Medical University, National Center for Children's Health, Beijing 100045, P.R. China

Received January 29, 2024; Accepted July 8, 2024

DOI: 10.3892/ol.2024.14653

Abstract. Uveal melanoma is the most common intraocular malignant tumor in adults. For patients presenting with cataracts and glaucoma, it is recommended to assess whether an intraocular lesion is present as the primary cause. The present study describes the case of a 52-year-old man with primary intraocular malignant melanoma. The patient experienced painless vision loss in the right eye for 1 year, with recent onset of eye swelling and pain in the week prior to seeking medical attention. A slit-lamp examination revealed a shallow anterior chamber in the right eye, a visibly opaque lens and a faint reflection of the tumor surface in the vitreous humor. In addition, the intraocular pressure of this eye was >60 mmHg. Magnetic resonance imaging revealed a large tumor behind the lens measuring 16x18x14 mm. Pathological examination confirmed the diagnosis of malignant melanoma. No BRCA-associated protein-1 somatic mutation was detected, whereas germline mutations of MutL protein homolog 1, RAD54 like, and SWI/SNF related, matrix associated, actin dependent regulator of chromatin, subfamily a, member 4 were identified. Extensive systemic examination excluded the possibility that the tumors originated from another part of the body. The present case report highlights the crucial role of slit-lamp examination in the detection of ocular tumors. It is advocated that for patients presenting with cataracts, attention should be paid to the possibility of intraocular tumors. Meticulous slit-lamp microscopy may reveal a reflection of the surface of a malignant melanoma, preventing misdiagnosis.

Introduction

Ocular melanoma constitutes ~5% of all melanoma cases. Uveal melanoma is a rare and highly malignant intraocular tumor that predominantly affects adults. This type of cancer exhibits distinct differences in biological characteristics and clinical manifestations compared with cutaneous melanoma (1). The risk of developing metastasis for patients with uveal melanoma is much higher compared to patients with a primary cutaneous melanoma and can be >50% in high-risk tumors of the posterior uvea (2-4). Research indicates that the incidence of both melanoma and cataracts is associated with exposure to ultraviolet radiation (5). The clinical symptoms of uveal melanoma often depend on the location and volume of the tumor (6), with early peripheral tumors being asymptomatic and frequently discovered during routine examinations. Most patients typically present with painless loss of vision or changes in vision, such as visual distortion or visual field defects. Fundoscopic examination may reveal the presence of an orange-red pigment or extensive serous retinal detachment, supporting the diagnosis of uveal melanoma (7). Uveal melanoma is known for its high malignancy, substantial metastatic potential and poor overall survival rates (8).

Uveal melanoma mainly occurs in the Caucasian population, while its incidence rate in various regions of Asia is 0.2-0.6 per million. The age at presentation for the Asian population is commonly 40-55 years, which is younger than that of Caucasian individuals, who have a mean age of 58 years at presentation (9). Uveal melanoma is the most common intraocular malignant tumor in adults, with 90% of cases of uveal melanoma occurring in the choroid, 6% in the ciliary body and 4% in the iris (8). Of note, the incidence of ocular melanoma is higher in males than in females (10). As the tumor grows, it may disrupt the nutrition or metabolism of the lens; furthermore, expansion of the tumor can push the lens-iris diaphragm forward, compressing the anterior chamber angle and the trabecular meshwork. In addition, cells or pigments shed by the tumor may enter the vitreous and aqueous humor and block the anterior chamber angle (11), leading to the development of complicated cataracts and secondary glaucoma.

The present study describes a typical case where the growth of the melanoma resulted in complicated cataracts and secondary glaucoma. Notably, slit-lamp examination revealed a reflection of the tumor surface. The present case report emphasizes the importance of careful slit-lamp examination for the detection of anterior segment tumors, and suggests

Correspondence to: Dr Sheng Su, Eye Hospital, The First Affiliated Hospital, Harbin Medical University, 23 Youzheng Street, Nangang, Harbin, Heilongjiang 150001, P.R. China
E-mail: shengsuhmu@126.com

Key words: uveal melanoma, complicated cataracts, secondary glaucoma, slit-lamp examination, BRCA-associated protein-1

that the presence of intraocular lesions should be evaluated in patients presenting with cataracts and glaucoma.

Case report

A 52-year-old Chinese man presented at the First Affiliated Hospital of Harbin Medical University (Harbin, China) in November 2023 with painless sharp vision loss in the right eye over the previous year, accompanied by eye swelling and pain in the week prior to seeking medical attention. The patient had only light perception in the right eye but normal visual acuity in the left eye. The left eye had an intraocular pressure of 15 mmHg, while the right eye had an intraocular pressure of >60 mmHg. A slit-lamp examination revealed extensive black pigmentation near the iris root at 4-6 o'clock in the right eye and in other scattered areas of the iris, with a shallow anterior chamber (Fig. 1A and B). In addition, the lens clearly exhibited white opacity (Fig. 1A). Notably, a reflective band was faintly visible behind the lens on the nasal side, suggesting the possibility of intraocular occupancy (Fig. 1C). Mild partial cataracts could be seen in the left eye, and no abnormal black pigment was found on the surface of the iris (Fig. 1D and E).

Ultrasound biomicroscopy of the right eye showed a shallow anterior chamber, bulging of the iris and a closed anterior chamber angle. The lens-iris diaphragm was displaced anteriorly (Fig. 2A), and a tumor was discovered in the ciliary body and choroid, which altered their structure (Fig. 2B and C). B-ultrasound and color Doppler ultrasound examinations revealed a hemispherical solid mass contiguous with the eyeball wall, with clear boundaries (Fig. 3). Orbital magnetic resonance imaging (MRI) demonstrated a T1 hyperintense, T2 hypointense lesion extending into the vitreous cavity from the lower part of the right eye. Due to the paramagnetic nature of melanin in tumors (12), MRI often exhibits characteristic features, namely high signal on T1WI and low signal on T2WI, which is different from most tumors that show a low to medium signal on T1WI and a medium to high signal on T2WI (13,14). These MRI features were strongly suggestive of malignant melanoma (Fig. 4). The lesion measured 16x18x14 mm and was closely associated with the posterior lens. Subsequent extensive systemic examinations, including brain, chest and abdominal CT scans, digestive and urological ultrasound scans, and positron emission tomography/CT-MRI, revealed no primary tumors in other parts of the body, which excluded the possibility of metastasis (Figs. S1-S3).

Eye enucleation surgery was performed, and the eye was histopathologically examined (Fig. 5). The tumor tissue appeared black to the naked eye (Fig. 5A) and was large in size (apical height, 16 mm; largest basal diameter, 24 mm). The tumor invaded the choroid (Fig. 5B and C), ciliary body and iris. The tumor tissue exhibited a high melanin content and a clear boundary with the surrounding normal uvea (Fig. 5D). Part of the adjacent uvea was deformed by tumor compression (Fig. 5E). The tumor was in close contact with the inner surface of the sclera (Fig. 5F) and the interior of the tumor was uneven (Fig. 5G). At a higher magnification, tumor cells and pigments were clearly visible in the histological images (Fig. 5H). The tumor cells were mainly poorly differentiated epithelioid cells with a small number of spindle cells (Fig. 5I). Immunohistochemical staining (supplementary materials of immunohistochemical methods) demonstrated that the number of Ki67-positive cells in the tumor tissue was markedly higher than that in normal tissue, although the melanin within the tumor impeded clear identification of the staining (Fig. 5J-L). BRAF gene mutation testing gave a negative result, showing that wild-type BRAF gene was present. In addition, a panel of 68 genes, named as homologous recombination repair genes (supplementary materials of genes), was analyzed by second-generation sequencing (BGI Genomics Co., Ltd.). The results showed the absence of a somatic BRCA-associated protein-1 (BAP1) mutation, whereas germline MutL protein homolog 1 (MLH1) mutation c.283T>G, RAD54 like (RAD54L) mutation c.1170-8T>C and SWI/SNF related, matrix associated, actin dependent regulator of chromatin, subfamily a, member 4 (SMARCA4) mutation c.2123+20G>T were detected (Table I). The patient underwent enucleation surgery and the incision gradually healed. At three weeks after surgery, the conjunctiva was relatively smooth and no residual black tissue was found by slit lamp microscopy observation, and no distant metastasis was found during the examination. The patient decided to not have any other treatments and planned to undergo regular physical examinations to detect possible metastases.

Discussion

In the present case, the patient initially only had painless vision loss, similar to that associated with cataracts, with mild eye swelling and pain that presented ~1 week before the patient sought medical attention. This indicates that patients may notice the condition at a late stage and then seek medical care. The tumor size was large according to the Collaborative Ocular Melanoma Study (COMS) classification (15), as it exceeded the dimensions of a medium tumor in this classification standard, defined as an apical height of 2.5-10 mm and largest basal diameter of ≤16 mm. A study by Liu *et al* (16) found that medium-sized tumors are most commonly detected, comprising 78% of cases, with large-sized tumors being less common and small-sized tumors being rare. Tumor size at the time of treatment has been indicated to be the most important factor associated with patient survival (17). According to the modified Callender's classification of uveal melanoma (18), the tumor in the present case, with its large proportion of epithelioid cells and small proportion of spindle cells, was mixed-cell type. Studies performed in India (19,20) and China (16) indicate that the incidence of spindle type tumors is higher than that of mixed cell-type tumors. Tumors with few epithelioid cells are generally associated with a slightly improved prognosis than tumors with more abundant epithelioid cells; however, one study found that tumors composed of 1-50% epithelioid cells had the same prognosis as tumors composed predominantly of epithelioid cells (18). A large volume and a large number of epithelioid cells indicate the probability of a higher mortality rate (17). The most notable characteristic of the present case was the concurrent involvement of the choroid, ciliary body and iris, with multi-regional involvement of the iris. A large study from China previously reported iris involvement in only 0.2% of uveal melanoma cases (9). The COMS trials reported

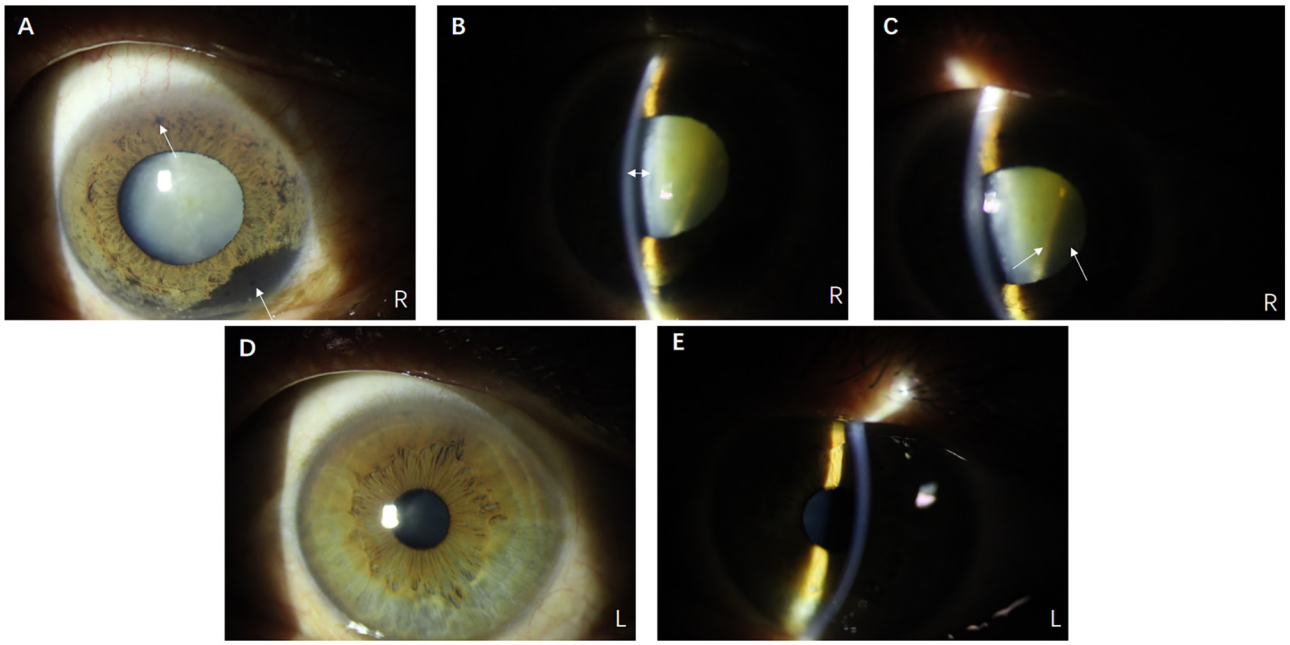

Figure 1. Slit-lamp microscopic images of the eye. (A) Diffuse illumination image of the right eye, showing prominent white opacities in the lens, extensive dark coloration at the 4-6 o'clock iris periphery and numerous scattered dark areas in other parts of the iris, as indicated by arrows. (B) Slit-lamp microscopic image of the shallow anterior chamber of the right eye. (C) Slit-lamp image showing a reflection of the surface of the tumor in the vitreous humor. (D) Diffuse illumination image of the left eye, depicting localized opacities in the lens. (E) Slit-lamp microscopic image of the left eye, showing a normal depth of the anterior chamber. R, right; L, left.

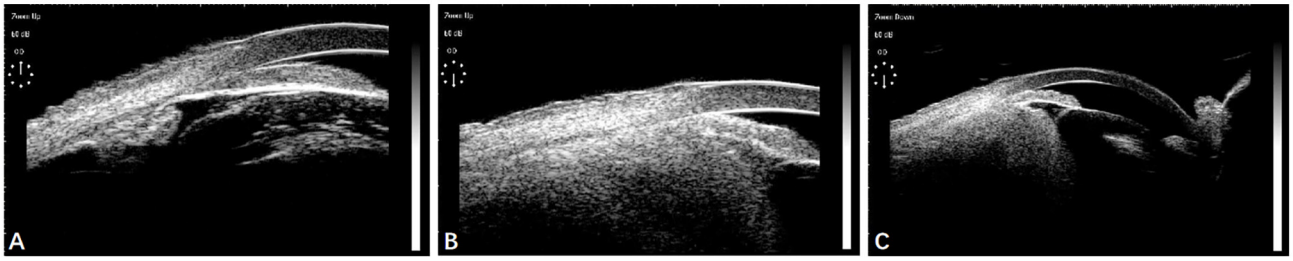

Figure 2. Ophthalmic UBM examination images. (A) UBM image of the right eye at the 12 o'clock position, showing a closed anterior chamber angle with no apparent tumor. UBM images of the right eye at the 6 o'clock position, showing (B) a closed angle and a ciliary body tumor and (C) compression of the lens by the tumor. UBM, ultrasound biomicroscopy.

5- and 10-year cumulative metastasis rates of 25 and 34% respectively, with 80% of the patients with metastasis dying within 1 year and 92% within 2 years after the diagnosis of metastases (21). In >90% of patients, metastases involve the liver. Other sites of metastasis include bone (29%) and the lungs (29%) (22). The largest tumor basal diameter and ciliary body involvement have been shown to be associated with metastasis and mortality (23). The average time from diagnosis to metastasis in Asian patients is reported to be 35 months (9). Despite the lack of distant metastases in the present case, lifelong follow-up is necessary.

Ocular ultrasound is valuable for the diagnosis of uveal melanoma, with characteristic findings of a hemispherical or mushroom-shaped solid mass contiguous with the eye wall (24). The tumor may appear hollow when imaged, consistent with the ultrasound findings in the present case. Additionally, the unique MRI characteristics of choroidal melanoma, which include high-signal intensity on T1-weighted imaging and low-signal intensity on T2-weighted imaging, contribute to significant contrast on the corresponding weighted images (25), aligning with the findings in the current case.

Tumor compression of the lens, invasion of the lens capsule or local circulatory disturbances due to tumor-derived products can lead to nutritional or metabolic disorders in the lens, causing cataracts. It has been suggested that tumor cells can express high levels of transforming growth factor-β and other cytokines, thereby promoting the development of cataracts (26). In addition, infiltration of the tumor into the anterior chamber angle can disrupt normal circulation of the aqueous humor, subsequently hindering aqueous outflow and causing a sustained increase in intraocular pressure (27), leading to secondary glaucoma. In the present case, a slit-lamp examination not only confirmed the presence of cataracts and a closed anterior chamber angle, but also, even in the presence of a visibly opaque lens, allowed a faint reflection of the tumor surface to be observed through the lens.

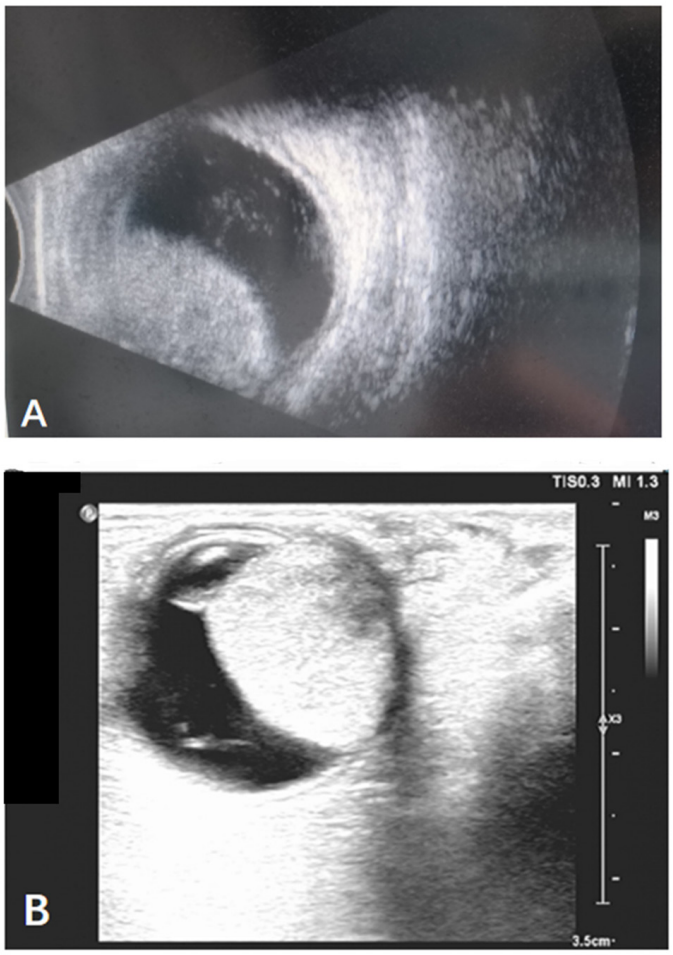

Figure 3. Ophthalmic B-scan and color Doppler ultrasound examination images. (A) B-scan ultrasound image of the right eye, showing a hemispherical mass in the vitreous cavity. (B) Ultrasound image of the right eye, depicting a solid intraocular mass compressing the lens, with clear boundaries.

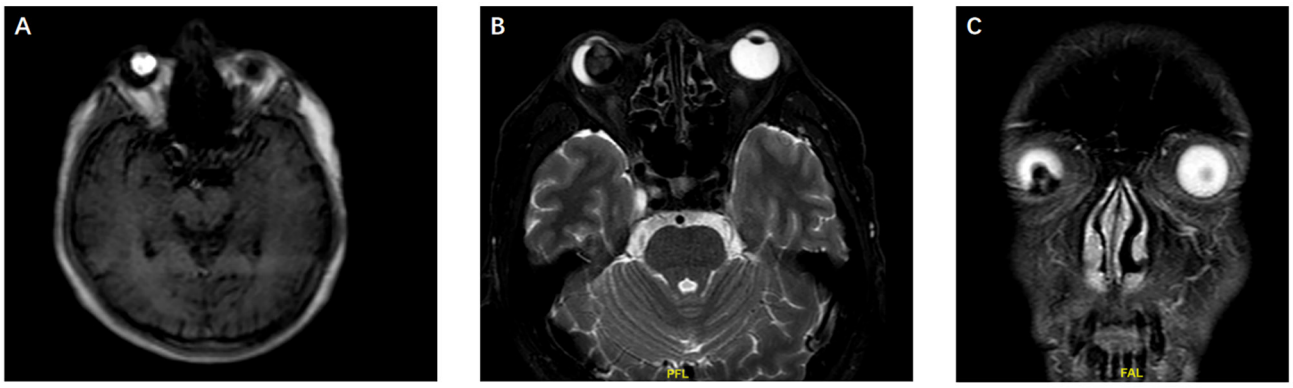

Figure 4. Orbital MRI plain scan images. (A) Transverse T1-weighted MRI image of the right eye, depicting a high signal lesion extending into the vitreous cavity. (B) Transverse T2-weighted MRI image of the right eye, depicting a low signal lesion extending into the vitreous cavity. (C) Coronal T2-weighted MRI image of the right eye, illustrating the low signal lesion. MRI, magnetic resonance imaging; FAL, foot direction; PFL, posterior.

Primary uveal melanoma can be classified into two subgroups based on gene expression profiling: Class I, which is associated with a low metastatic risk, and class II, which is associated with a high metastatic risk (28). BAP1 has been shown to be mutated in ~40% of patients with uveal melanoma (29). Of note, in metastatic uveal melanoma, BAP1 mutations are detected in up to 80% of cases, which suggests that BAP1 inactivation is an important contributor to disease progression (30,31). BAP1 modulates chromatin-associated processes, including gene expression, DNA replication and DNA repair, and contributes to the activation of regulatory immune cells; therefore, its loss is associated with the suppression of immune responses and increased tumor immune evasion (32). In the present case, neither somatic nor germline BAP1 mutations were identified. However, three homologous recombination repair gene mutations affecting other genes,

Table I. Results of the detection of germline variations in tumor susceptibility genes.

Gene name	NM number	Nucleotide changes	Functional changes	Mutation type[a]
SMARCA4	NM_001128849.1	c.2123+20G>T	Splice	Unknown significance
RAD54L	NM_003579.3	c.1170-8T>C	Splice	Unknown significance
MLH1	NM_000249.3	c.283T>G	Missense	Unknown significance

No somatic variations in tumor susceptibility genes were detected. [a]Genetic variation is divided into five levels: Known pathogenic variation, suspected pathogenic variation, unknown significance variation, suspected benign variation and benign variation. SMARC4, SWI/SNF related, matrix associated, actin dependent regulator of chromatin, subfamily a, member 4; RAD54L, RAD54 like; MLH1, MutL protein homolog 1.

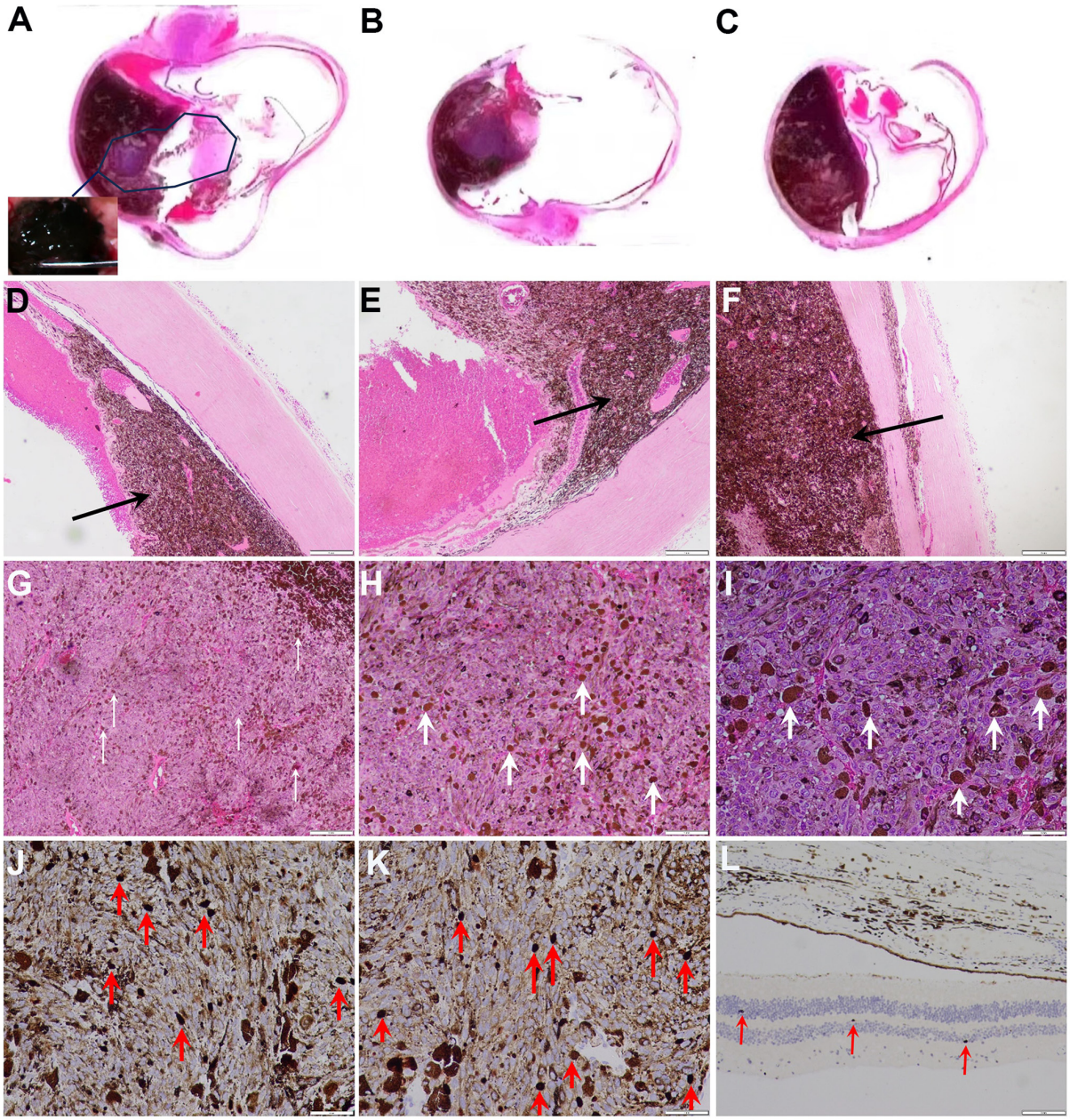

Figure 5. Histological and pathological examination results. (A) Extracted eyeball and tumor morphology. The inset in A shows that the tumor in the eye is black (magnification, x5). (B) Section and tumor morphology of the eyeball (magnification, x5). (C) Another section of the eyeball and tumor morphology (magnification, x5). (D) Tumor invasion near the normal uvea. (E) Tumor compresses the uvea. (F) Tumor tissue is present on the inner surface of the sclera (magnification in D-F, x40; scale bar, 0.25 mm; the tumor tissue is indicated by black arrows). (G) Uveal melanoma tumor cell morphology. Pigmented tumor cells are indicated by white arrows. Most of the tumor cells were epithelioid cells (magnification, x40; scale bar, 0.25 mm). (H) Higher magnification image of G (magnification, x100; scale bar, 0.1 mm) and (I) a further magnified image (x200; scale bar, 0.05 mm). Ki67 immunohistochemical results of (J and K) tumor tissue (magnification, x200; scale bar, 0.05 mm) and (L) normal tissue (magnification, x100; scale bar, 0.1 mm). There were markedly more Ki67-positive cells in the tumor tissue than in normal tissue. Ki67-positive cells are indicated by red arrows.

namely MLH1, RAD54L and SMARCA4, were detected. SMARCA4 deficiency has been shown to be a synthetic lethal factor when combined with CDK4/6 inhibition (33), and high levels of SMARCA4 expression are associated with poor prognosis in numerous types of tumors, including liver hepatocellular carcinoma, and kidney renal clear cell carcinoma (34). The nonrandom deletion of RAD54L is associated with significant heterogeneity in the malignant progression of tumors such as melanoma (35). In the present case, a missense mutation in the MLH1 gene, a mismatch repair (MMR) gene was observed. Notably, the detection of high-frequency microsatellite instability/MMR deficiency is increasingly being included in the routine tumor treatment of patients with various types of advanced solid tumors (36). This is driven by several key reasons: i) The microsatellite instability (MSI)/MMR status can significantly influence treatment decisions; ii) major oncology societies, including the National Comprehensive Cancer Network (NCCN) and the European Society for Medical Oncology (ESMO), now recommend MSI/MMR testing as part of routine assessment in specific types of solid tumors; iii) beyond guiding treatment choices, the MSI/MMR status serves as a prognostic indicator. However, whether these three gene mutations have a role in the pathogenesis of uveal melanoma requires further study.

Although ~99% of patients with ocular melanoma exhibit no evidence of systemic metastatic disease at the initial diagnosis, patients may develop metastases at any time thereafter, with the liver being the most common site (37). Therefore, regular monitoring is crucial in the follow-up of patients with ocular melanoma. The treatment choices for uveal melanoma vary according to tumor size, and the most frequently used modalities are enucleation and focal radiotherapy, particularly plaque therapy (38-42). With regard to programmed cell death protein 1 (PD-1) and programmed death ligand 1 (PD-L1) expression, uveal melanoma most frequently has $PD\text{-}1^{-}/PD\text{-}L1^{-}$ or $PD\text{-}1^{+}/PD\text{-}L1^{-}$ status, which indicates immunological tolerance, with the absence or functional suppression of tumor-infiltrating lymphocytes in the tumor microenvironment, respectively (43). This may explain why uveal melanoma exhibits a poor response to anti-PD-1 therapy (44). Uveal melanoma is also associated with high expression of glycoprotein 100 (gp100), melanoma-associated antigen, melanoma antigen recognized by T cells and tyrosinase-related protein-1, which are known to be immunogenic cancer antigens (45-47). Therefore, these may represent targets for uveal melanoma therapy. For instance, tebentafusp, also known as IMCgp100, a bispecific fusion protein directed against gp100, has been approved by the FDA for unresectable or metastatic uveal melanoma.

In conclusion, ocular melanoma is the most common primary intraocular malignant tumor in adults, and cataracts and glaucoma can be secondary manifestations of intraocular primary lesions. Slit-lamp examination may reveal the presence of tumor cells as localized areas of black pigmentation in the iris, and may also show reflections and shadows of the tumor. Therefore, slit-lamp examination is essential for the preliminary diagnosis of ocular tumors.

Acknowledgements

Not applicable.

Funding

This study was supported by grants from the National Natural Science Foundation of China (grant no. 81800811) and the Outstanding Young Medical Talent Training Funding Project of the First Affiliated Hospital of Harbin Medical University (grant no. 2021J13).

Availability of data and materials

The high-throughput sequencing data generated in the present study may be found in the China National Center for Bioinformation under accession number HRA007562 or at the following URL: (https://ngdc.cncb.ac.cn/search/specific?db=hra&q=HRA007562). The other data generated in the present study may be requested from the corresponding author.

Authors' contributions

YW conceived the study and wrote the manuscript. QSun and ZL designed the study and assisted with the drafting of the manuscript. XH and QSu collected data from imaging examinations and participated in histological and morphological detection. SS revised the manuscript and made substantial contributions to the design of the study. FL designed the gene tests, analyzed the mutation results and participated in revision of the manuscript. SS and YW confirm the authenticity of all the raw data. All authors read and approved the final version of the manuscript.

Ethics approval and consent to participate

The present study was conducted according to the guidelines of the Declaration of Helsinki. Written informed consent was obtained from the patient.

Patient consent for publication

Written informed consent was obtained from the patient for publication of the data and images in this case report.

Competing interests

The authors declare that they have no competing interests.

References

1. Bol KF, Donia M, Heegaard S, Kiilgaard JF and Svane IM: Genetic biomarkers in melanoma of the ocular region: What the medical oncologist should know. Int J Mol Sci 21: 5231, 2020.
2. Singh AD, Turell ME and Topham AK: Uveal melanoma: Trends in incidence, treatment, and survival. Ophthalmology 118: 1881-1885, 2011.
3. Kujala E, Mäkitie T and Kivelä T: Very long-term prognosis of patients with malignant uveal melanoma. Invest Ophthalmol Vis Sci 44: 4651-4659, 2003.
4. Jensen OA: Malignant melanomas of the human uvea: 25-year follow-up of cases in Denmark, 1943--1952. Acta Ophthalmol (Copenh) 60: 161-182, 1982.
5. Varssano D, Friedman M, Goldstein M, Bar-Sela S, Sella T, Shalev V and Chodick G: Association between cataract and keratinocytic skin cancers or melanoma: Speculating on the common role of sun and ultraviolet radiation exposures. Ophthalmic Epidemiol 24: 336-340, 2017.

6. Fish GE, Jost BF, Snyder WI, Fuller DG and Birch DG: Cataract extraction after brachytherapy for malignant melanoma of the choroid. Ophthalmology 98: 619-622, 1991.
7. Factors predictive of growth and treatment of small choroidal melanoma: COMS Report No. 5. The Collaborative Ocular Melanoma Study Group. Arch Ophthalmol 115: 1537-1544, 1997.
8. Shields CL, Furuta M, Thangappan A, Nagori S, Mashayekhi A, Lally DR, Kelly CC, Rudich DS, Nagori AV, Wakade OA, *et al*: Metastasis of uveal melanoma millimeter-by-millimeter in 8033 consecutive eyes. Arch Ophthalmol 127: 989-998, 2009.
9. Manchegowda P, Singh AD, Shields C, Kaliki S, Shah P, Gopal L and Rishi P: Uveal melanoma in Asians: A review. Ocul Oncol Pathol 7: 159-167, 2021.
10. McLaughlin CC, Wu XC, Jemal A, Martin HJ, Roche LM and Chen VW: Incidence of noncutaneous melanomas in the U.S. Cancer 103: 1000-1007, 2005.
11. Weinreb RN, Aung T and Medeiros FA: The pathophysiology and treatment of glaucoma: A review. JAMA 311: 1901-1911, 2014.
12. Adam G, Brab M, Bohndorf K and Günther RW: Gadolinium-DTPA-enhanced MRI of intraocular tumors. Magn Reson Imaging 8: 683-689, 1990.
13. Gomori JM, Grossman RI, Shields JA, Augsburger JJ, Joseph PM and DeSimeone D: Choroidal melanomas: Correlation of NMR spectroscopy and MR imaging. Radiology 158: 443-445, 1986.
14. Peyster RG, Augsburger JJ, Shields JA, Hershey BL, Eagle R Jr and Haskin ME: Intraocular tumors: Evaluation with MR imaging. Radiology 168: 773-779, 1988.
15. Design and methods of a clinical trial for a rare condition: The collaborative ocular melanoma study. COMS report no. 3. Control Clin Trials 14: 362-391, 1993.
16. Liu YM, Li Y, Wei WB, Xu X and Jonas JB: Clinical characteristics of 582 patients with uveal melanoma in China. PLoS One 10: e0144562, 2015.
17. Diener-West M, Hawkins BS, Markowitz JA and Schachat AP: A review of mortality from choroidal melanoma. II. A meta-analysis of 5-year mortality rates following enucleation, 1966 through 1988. Arch Ophthalmol 110: 245-250, 1992.
18. McLean IW, Foster WD, Zimmerman LE and Gamel JW: Modifications of callender's classification of uveal melanoma at the armed forces institute of pathology. Am J Ophthalmol 96: 502-550, 1983.
19. Kashyap S, Venkatesh P, Sen S, Khanduja S, Shrey D, Tinwala S and Garg S: Clinicopathologic characteristics of choroidal melanoma in a north Indian population: Analysis of 10-year data. Int Ophthalmol 34: 235-239, 2014.
20. Meeralakshmi P, Shah PK and Narendran V: Experiences of two different modalities in the management of choroidal melanoma in the Asian Indian population. South Asian J Cancer 6: 134-136, 2017.
21. Diener-West M, Reynolds SM, Agugliaro DJ, Caldwell R, Cumming K, Earle JD, Hawkins BS, Hayman JA, Jaiyesimi I, Jampol LM, *et al*: Development of metastatic disease after enrollment in the COMS trials for treatment of choroidal melanoma: Collaborative ocular melanoma study group report no. 26. Arch Ophthalmol 123: 1639-1643, 2005.
22. Steckler AM, Francis JH, Shoushtari AN, Abramson DH and Barker CA: Uveal melanoma metastatic at initial diagnosis: A case series. Melanoma Res 32: 120-123, 2022.
23. Zhou N, Zhang R, Liu Y and Wei W: Clinical characteristics of UM and association of metastasis of uveal melanoma with congenital oculocutaneous melanosis in Asian patients: Analysis of 1151 consecutive eyes. Ophthalmol Retina 5: 1164-1172, 2021.
24. Jacobsen BH, Ricks C and Harrie RP: Ocular ultrasound versus MRI in the detection of extrascleral extension in a patient with choroidal melanoma. BMC Ophthalmol 18: 320, 2018.
25. Neupane R, Gaudana R and Boddu SHS: Imaging techniques in the diagnosis and management of ocular tumors: Prospects and challenges. AAPS J 20: 97, 2018.
26. Kase S, Parikh JG, Youssef PN, Murphree AL and Rao NA: Transforming growth factor beta in retinoblastoma-related cataract. Arch Ophthalmol 126: 1539-1542, 2008.
27. Camp DA, Yadav P, Dalvin LA and Shields CL: Glaucoma secondary to intraocular tumors: Mechanisms and management. Curr Opin Ophthalmol 30: 71-81, 2019.
28. Onken MD, Worley LA, Ehlers JP and Harbour JW: Gene expression profiling in uveal melanoma reveals two molecular classes and predicts metastatic death. Cancer Res 64: 7205-7209, 2004.
29. Field MG, Durante MA, Anbunathan H, Cai LZ, Decatur CL, Bowcock AM, Kurtenbach S and Harbour JW: Punctuated evolution of canonical genomic aberrations in uveal melanoma. Nat Commun 9: 116, 2018.
30. Harbour JW, Onken MD, Roberson ED, Duan S, Cao L, Worley LA, Council ML, Matatall KA, Helms C and Bowcock AM: Frequent mutation of BAP1 in metastasizing uveal melanomas. Science 330: 1410-1413, 2010.
31. Karlsson J, Nilsson LM, Mitra S, Alsen S, Shelke GV, Sah VR, Forsberg EMV, Stierner U, All-Eriksson C, Einarsdottir B, *et al*: Molecular profiling of driver events in metastatic uveal melanoma. Nat Commun 11: 1894, 2020.
32. Figueiredo CR, Kalirai H, Sacco JJ, Azevedo RA, Duckworth A, Slupsky JR, Coulson JM and Coupland SE: Loss of BAP1 expression is associated with an immunosuppressive microenvironment in uveal melanoma, with implications for immunotherapy development. J Pathol 250: 420-439, 2020.
33. Xue Y, Meehan B, Fu Z, Wang XQD, Fiset PO, Rieker R, Levins C, Kong T, Zhu X, Morin G, *et al*: SMARCA4 loss is synthetic lethal with CDK4/6 inhibition in non-small cell lung cancer. Nat Commun 10: 557, 2019.
34. Guerrero-Martínez JA and Reyes JC: High expression of SMARCA4 or SMARCA2 is frequently associated with an opposite prognosis in cancer. Sci Rep 8: 2043, 2018.
35. Ryu B, Kim DS, Deluca AM and Alani RM: Comprehensive expression profiling of tumor cell lines identifies molecular signatures of melanoma progression. PLoS One 2: e594, 2007.
36. Latham A, Srinivasan P, Kemel Y, Shia J, Bandlamudi C, Mandelker D, Middha S, Hechtman J, Zehir A, Dubard-Gault M, *et al*: Microsatellite instability is associated with the presence of lynch syndrome pan-cancer. J Clin Oncol 37: 286-295, 2019.
37. Balasubramanya R, Selvarajan SK, Cox M, Joshi G, Deshmukh S, Mitchell DG and O'Kane P: Imaging of ocular melanoma metastasis. Br J Radiol 89: 20160092, 2016.
38. Davidorf FH, Pajka JT, Makley TA Jr and Kartha MK: Radiotherapy for choroidal melanoma. An 18-year experience with radon. Arch Ophthalmol 105: 352-355, 1987.
39. Lommatzsch PK: Results after beta-irradiation (106Ru/106Rh) of choroidal melanomas. Twenty years' experience. Am J Clin Oncol 10: 146-151, 1987.
40. Gass JD: Comparison of prognosis after enucleation vs cobalt 60 irradiation of melanomas. Arch Ophthalmol 103: 916-923, 1985.
41. Augsburger JJ, Gamel JW, Sardi VF, Greenberg RA, Shields JA and Brady LW: Enucleation vs cobalt plaque radiotherapy for malignant melanomas of the choroid and ciliary body. Arch Ophthalmol 104: 655-661, 1986.
42. Augsburger JJ, Gamel JW, Lauritzen K and Brady LW: Cobalt-60 plaque radiotherapy vs enucleation for posterior uveal melanoma. Am J Ophthalmol 109: 585-592, 1990.
43. Rossi E, Schinzari G, Zizzari IG, Maiorano BA, Pagliara MM, Sammarco MG, Fiorentino V, Petrone G, Cassano A, Rindi G, *et al*: Immunological backbone of uveal melanoma: Is there a rationale for immunotherapy? Cancers (Basel) 11: 1055, 2019.
44. Javed A, Arguello D, Johnston C, Gatalica Z, Terai M, Weight RM, Orloff M, Mastrangelo MJ and Sato T: PD-L1 expression in tumor metastasis is different between uveal melanoma and cutaneous melanoma. Immunotherapy 9: 1323-1330, 2017.
45. de Vries TJ, Trancikova D, Ruiter DJ and van Muijen GN: High expression of immunotherapy candidate proteins gp100, MART-I, tyrosinase and TRP-I in uveal melanoma. Br J Cancer 78: 1156-1161, 1998.
46. de Vries TJ, Fourkour A, Wobbes T, Verkroost G, Ruiter DJ and van Muijen GN: Heterogeneous expression of immunotherapy candidate proteins gp100, MART-1, and tyrosinase in human melanoma cell lines and in human melanocytic lesions. Cancer Res 57: 3223-3229, 1997.
47. Luyten GP, van der Spek CW, Brand I, Sintnicolaas K, de Waard-Siebinga I, Jager MJ, de Jong PT, Schrier PI and Luider TM: Expression of MAGE, gp100 and tyrosinase genes in uveal melanoma cell lines. Melanoma Res 8: 11-16, 1998.